remote sensing

MDPI

Article

Assessing the Volume of Defensive Structures for Architectural Energetics Analysis Using 3D Electrical Resistivity Tomography

Radek Klanica [1,*], Hana Grison [1], Jindřich Šteffl [2] and Roman Beránek [1]

[1] Institute of Geophysics of the CAS, Boční II/1401, 141 31 Prague, Czech Republic; grison@ig.cas.cz (H.G.); beranek@ig.cas.cz (R.B.)
[2] Regional Museum in Teplice, Zámecké Náměstí 14, 415 01 Teplice, Czech Republic; jindra.ul@post.cz
* Correspondence: rk@ig.cas.cz; Tel.: +420-267-103-084

Abstract: Architectural energetics is a methodology that translates architectural objects into a quantitative time-labor equivalent, from which information about past societies, labor organizations, or political relations can be inferred. Preceding such study, the volume of every architectural structure must be determined. This is usually done by in situ measurements and computing of volume by mathematical formulae or using UAV-based photogrammetry processed into digital surface model. However, both of these methods are impracticable in the case of buried or semi-buried monuments where the only remaining option is direct excavation. Hence, we introduce a new method for the determination of volumetric information based on the electrical resistivity tomography (ERT) geophysical method. We conducted our study at defensive lines (ramparts/ditches) within two hillforts of different ages, constructed from different building materials, in the Czech Republic. ERT surveys performed in 3D can differentiate ramparts/ditches in detail from the surrounding environment based on resistivity. Compared to previous excavations, the 3D inversion results show that ERT can obtain meaningful volumes based on the chosen resistivity threshold. The best results were achieved on homogeneous semi-buried ramparts and the ditch. ERT can be performed at a fraction of the cost of direct excavation. This method also leaves an intact site for future generations.

Keywords: electrical resistivity tomography; archaeological prospection; geophysics; hillfort; architectural energetics; volume

Citation: Klanica, R.; Grison, H.; Šteffl, J.; Beránek, R. Assessing the Volume of Defensive Structures for Architectural Energetics Analysis Using 3D Electrical Resistivity Tomography. *Remote Sens.* **2022**, *14*, 2652. https://doi.org/10.3390/rs14112652

Academic Editors: Geert Verhoeven and Gabriel Vasile

Received: 6 April 2022
Accepted: 31 May 2022
Published: 1 June 2022

1. Introduction

All human societies have created remarkable architectural monuments that tell us about their way of life. For these reasons, architecture is one of the most studied elements from past societies in both anthropological and classical archaeology. One category of architectural analysis involves discerning specific types of labor organizations, offering deeper insight into engineering skills, political power, and especially the scale of labor. By quantifying the number of laborers per building task, we can estimate the total construction costs and enter into the archeological field of architectural energetics [1].

Architectural energetics [2–4] involves translating architectural objects into their quantified time-labor equivalent, which can subsequently be used for inferring information about past societies, labor organizations, or political and social relations. Several methodological steps must be completed to acquire such knowledge. Firstly, the analyzed structure must be deconstructed into measurable parts, usually according to material, e.g., stone components are distinguished from wooden, etc. Secondly, the volume of every component must be determined [5]; however, measuring the original volume of the archaeological structure is an imprecise and difficult task. For example, the volume of ramparts and ditches is often altered by natural processes or, similarly, walls and stone buildings must be recovered from collapsed material. Thirdly, the architectural component's labor cost involves procuring raw material, transportation to the construction site, and the actual

assembly of the architectural object. Finally, the labor cost translates into time-labor units as person-days (p-d) or person-hours (p-h), expressing the approximate length of time to build such a structure by one person [1].

As described in the second step, volume can be determined using multiple approaches. The simplest method is based on in situ object measurements and volume derived from mathematical formulae. An accurate approach for estimating the volume of surface objects is using unmanned aerial vehicle (UAV)-based photogrammetry processed into a digital surface model [6]. However, in the case of buried or partially buried objects, these estimates rely on excavations, which can cause irreversible destruction to the archaeological site. Databases containing 3D virtual models (e.g., CyArk; UCLA digital Karnak; Learning sites) can be used for well-preserved monuments.

Geophysical methods in archaeology are usually used as non-invasive tools for imaging various archaeological features [7,8]. Dense 3D surveys assess volumetric information, such as the size of ore deposits [9] or the volume of archaeological layers [10]. There are ideal geophysical methods that deliver direct vertical information, such as electrical resistivity tomography (ERT) or different electromagnetic methods (frequency domain electromagnetics, ground-penetrating radar [11,12]).

ERT can characterize the subsurface distribution of electrical resistivity in lateral and vertical directions (by 2D or 3D surveys) and distinguish various archaeological features such as walls, pits, ditches, burial mounds, or foundations from the surrounding environment [13–17]. In principle, electrical current I (A) is injected into the ground through two steel electrodes (C1 and C2), while the potential difference U (V) is measured between another pair of electrodes (P1 and P2). By considering the geometry factor of the electrode array k, the resistivity can be obtained through a modified Ohm's law, $\rho(\Omega m) = kU/I$. The depth range of the ERT depends on the distance of current electrodes C1 and C2 and on the separation between C1C2 and P1P2 couples. The investigation depth of the most common electrode, the Wenner–Schlumerber array, is given by C1C2/5. The resolution of the method is given by electrode spacing [18]. In a homogeneous halfspace, ρ would be the true resistivity; however, due to resistivity heterogeneities, ρ yields apparent resistivity ρ_a. The apparent resistivity must subsequently be converted to the (true) subsurface resistivity by an inversion process, which attempts to find a resistivity model to explain the measured data. This process is performed through iterative non-linear regularized inversion algorithms [19] conducted in different programs (e.g., Res2Dinv, BERT) in 2D (profile) or 3D (cube). The inversion process adjusts the model parameters to minimize a norm, expressing the difference between the modeled and observed data using the L1 norm (so-called robust inversion), which favors sharp contrasts, or the L2 norm (standard inversion) and smooth transitions between individual model cells (for using different norms, e.g., Loke et al. [20]).

Based on resistivity, the contrast between the targeted structure and the surrounding environment reveals the resistivity boundary by which objects of interest are limited and extracted from the resistivity model. Subsequently, the volume of such model parts can be easily computed. We chose defensive lines (ramparts/ditches) between two hillforts of different ages and building materials in the Czech Republic as a target. The calculated volumes are discussed with respect to ERT inversion settings and compared with archaeological excavations. Our study introduces a new approach for obtaining volumetric information about buried or semi-buried archaeological objects such as ramparts, ditch infills, or building foundations using 3D ERT surveys. Moreover, we intend to compare our results to previous archaeological knowledge based on excavations.

2. Study Sites

2.1. Hillfort Hradišťany

The highest-lying hillfort from the Bronze Age epoch in Bohemia is located on a plateau of the vast mountain massif Hradišťany (752 m a.s.l.; GPS 50.5074N, 13.8702E; Figure 1A), which is part of the České středohoří Mts. volcanosedimentary complex mainly

built by Tertiary alkaline volcanics with sedimentary intercalations [21]. The main body of the Hradišťany hill is built by phonolites of Ústí and Dobrná Fm. (36–19 Ma) and is covered in its uppermost parts by sands of Most Fm. (28–16 Ma) together with basanitic lavas from Štrbice Fm. (10–9 Ma; [22]).

The hillfort covers the hilltop, which rises from the surrounding landscape at an elevation difference of almost 300 m on the northern side and about 200 m in other directions. The summit plateau is longer along the west–east and slants slightly northward. It is naturally protected on all sides by either steep slopes or rocky cliffs [23]. The hillfort has a two-part layout and comprises an outer rampart that delimits the bailey, and an inner rampart enclosing the acropolis without any outer ditch. The hillfort covers an area of 7 ha, and the bailey and acropolis cover areas of 3.5 ha each (Figure 1C).

Like the inner rampart, the outer rampart was built with dry-stacked stones (local basalts) at a length of 813 m. Compared to the inner rampart, it lies lower and surrounds it from the west, north, and east directions. The outer and inner ramparts are connected at the SW and SE sides of the acropolis, leaving the southern side protected only by the inner rampart. The maximum width of the preserved outer rampart remains is 3.7 m, and the height is 0.8 m. Currently, the inner rampart is between 6 and 9 m wide and from 1 to 2.4 m high [24], with a total length of 698 m. According to the excavations of Šolle and Váňa [25] (Figure 1B), the original width of the inner rampart was ca. 3.3 m, and it had a minimum height of 2 m [25,26]. Therefore, the total volume of a 1-m-wide strip of rampart contained ca. 6.6 m^3 of rock material.

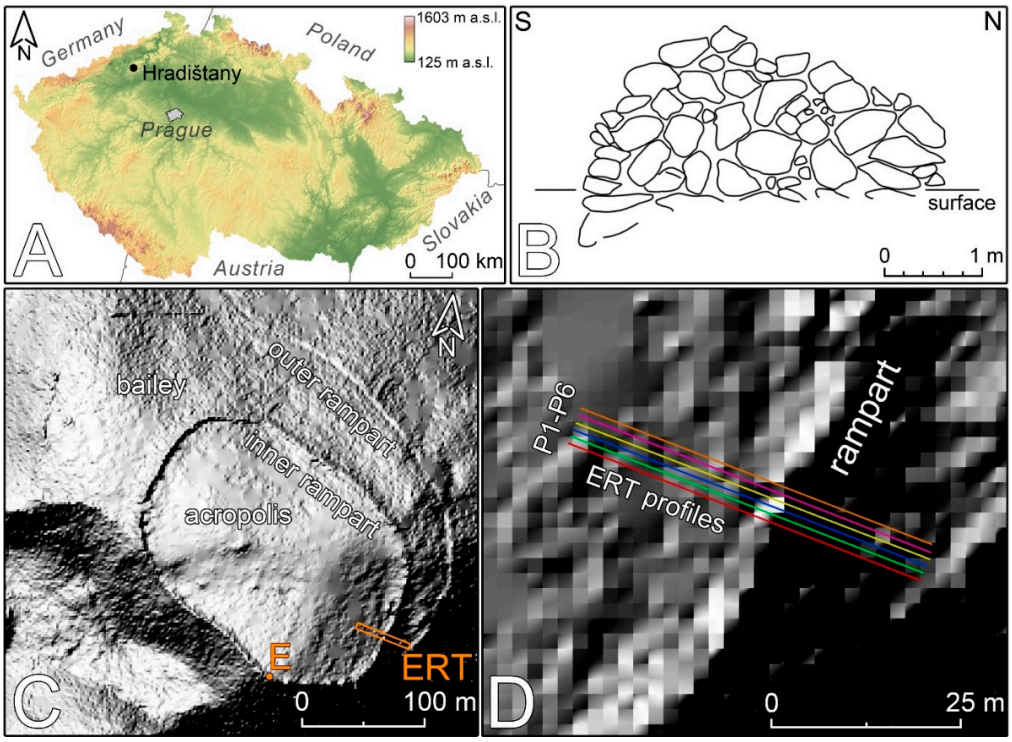

Figure 1. (**A**) Position of the hillfort Hradišťany in the Czech Republic. (**B**) Sketch of the rampart cross-section excavated in 1951 (redrawn after Šolle and Váňa [25]). (**C**) Digital elevation model of hillfort Hradišťany with excavation positions "E" and the area measured by ERT. (**D**) Magnified area of ERT measurements with measured profiles.

The hillfort was inhabited during the Young Bronze Age (ca. 1300–1000 BC), based on excavated artifacts including pottery, a bronze knife with a frame handle, and three bronze axes. A few artifacts suggest that an even older settlement (Middle Bronze Age) was once based on the Hradišťany hill [27].

2.2. Hillfort Královice

Hillfort Královice is located on a distinct promontory above the Rokytka river and is bordered by steep slopes from the west and south, reaching up to 30 m of elevation difference; the northern and eastern sides are protected by two north–south-oriented defensive lines (GPS 50.0444N, 14.6321E; Figure 2A). The basement of the locality is represented by sea sediments of the Barrandian Proterozoic (Štěchovice Group), mainly built by siltstones, shales, and greywackes, which are covered by Quaternary loess. The hillfort can be divided into two parts: the bailey area of ca. 3.7 ha with an outer rampart, and the ditch, which is delimited by a transverse rampart from the acropolis, covering an area of ca. 2.4 ha (Figure 2C).

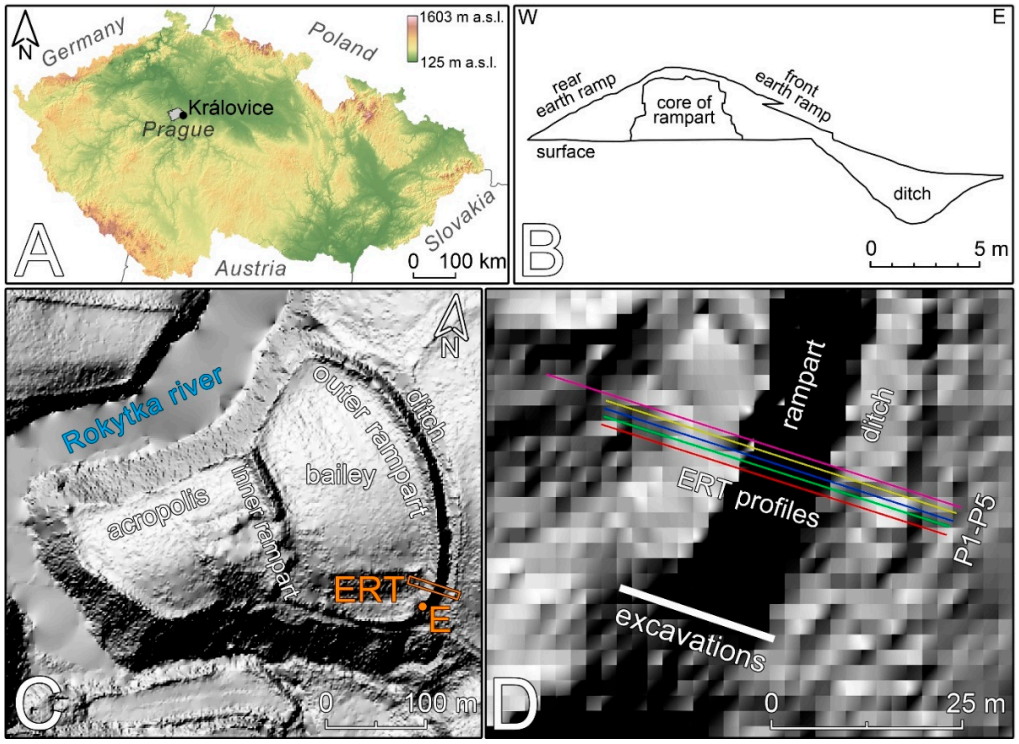

Figure 2. (**A**) Position of the hillfort Královice in the Czech Republic. (**B**) Sketch of the outer defensive line cross-section excavated in 2012 (redrawn after Štefan and Hasil [28]). (**C**) Digital elevation model of hillfort Královice with excavation positions "E" and measured area by ERT. (**D**) Magnified area of ERT measurements with measured and excavated profiles.

The outer rampart is preserved at a length of 335 m, a width between 15 and 20 m, and a height from 3 to 4 m. In front of the rampart was the ditch, which is currently altered by erosional processes, and a younger sunken lane. The outer defensive line was excavated in 2012 by Štefan and Hasil [28], while the results helped reconstruct individual building phases and materials used (Figure 2B). In the first phase, the fortification was built as a wood-and-earth rampart with a wooden frame. Loess material, probably dug from the ditch, was used as the main construction material. The rampart was approximately 5 m wide and at least 2.8 m high, with a stone screen wall adjoined to the front and rear wooden wall at the back (Figure 2B). The acquired dimensions suggest that a 1-m-wide strip across the rampart was built from 14 m^3 of material. The ditch in front of the rampart was probably already present; however, its precise appearance is unknown. The rampart was later modified by an earth ramp without an interior wooden frame on both sides of the original core. A dry-stack screen wall securing the original core was probably disassembled and rebuilt at the crown of the front side of the rampart using stone from the original screen wall. Currently, the eroded remains of screen wall stones fill the ditch at a depth of ca. 4.2 m, suggesting later destruction of the defensive system. The inner transverse

rampart had a length of around 170 m; however, it is preserved only at a length of 84 m with a width of ca. 10 m and a height of 2.2 m [28].

The hillfort was first inhabited between the end of 9th century and the middle of the 10th century. It was abandoned at the turn of the 12th and 13th centuries. This timeline is supported by ceramic artifacts and excavated objects (pits, etc.; [28]).

3. Materials and Methods

3.1. Field Setup

ERT data were collected using a five-channel ARES II resistivity system (GF Instruments, Brno, Czech Republic) with a high-density (HD) version of the inverse Wenner–Schlumberger electrode array [29]. The HD version of a particular array refers to arrangement with a larger number of measured points (ca. double) than in the case of regular non-HD arrays. This is achieved by using overlapping data levels with different combinations of distances between C1–C2 and P1–P2 electrodes [29]. The inverse Wenner–Schlumberger array was chosen based on tests of different electrode arrays within similarly constructed hillforts [15], where it performed better than the dipole–dipole array. Additionally, inverse Wenner–Schlumberger allows multi-channel acquisition, compared to the traditional Wenner–Schlumberger array, and decreases the time required for measurements. A so-called quasi-3D survey [17] was conducted on both investigated sites, which consisted of multiple parallel lines acquired from 2D profiles and subsequently merged into a joint dataset for 3D inversion. The precise position of each profile was obtained with a GNSS Trimble R10 GPS receiver, while the topography of the entire measured grid was extracted from LiDAR digital elevation models with height mean error of 0.18 m [30].

The inner rampart of hillfort Hradišťany was covered by six profiles that were 31 m long, with a line and electrode spacing of 1 m (covering a part of the rampart 5 m wide; Figure 1D). Since the ground contact resistance of the electrodes was around 20 kΩ in the stony rampart, each measurement was stacked minimally eight times to ensure sufficient data quality. The outer rampart of hillfort Královice was covered by four profiles that were 39 m long, plus one 55-m-long profile, with a line and electrode spacing of 1 m (covering a part of the rampart 4 m wide; Figure 2D).

3.2. Data Processing and Modelling

Acquired data were preprocessed and analyzed for errors in several ways before the inversion. From the ARES II instrument were downloaded only data points with standard deviation less than 10%. This first step reduced total number of measured points only about units of points. The second step included running preliminary 2D inversions in Res2Dinv software, which make it possible to assess RMS error statistics. Points with higher errors than an intuitively selected threshold were deleted by this process, while edited data were saved in raw format for final inversions. This approach reduced number of measured points by about 8–10% in case of hillfort Hradišťany and about 3–4% in the case of hillfort Královice. In general, data quality from hillfort Hradišťany was lower, due to complications related to data acquisition in the stony rampart, while data from hillfort Královce showed very high quality. Subsequently, edited data were inverted with the Boundless Electrical Resistivity Tomography package (BERT2 [31–33]), every individual 2D profile, and subsequently, both localities in 3D. Since 2D inversions generally produce models with higher resolution and sharper anomalies [34], the 2D results were mainly used to delineate the body of the ramparts/ditch (choice of resistivity value) together with the on-site situation and excavations. Later, a set of 3D inversion runs with different parameters (e.g., regularization weights, quality of the surface mesh, size of the cells of the model) were conducted to evaluate changes in the 3D model caused by different inversion settings. Choice of these parameters directly affects the convergence of the inversion process and the resulting RMS error (for further explanation of individual parameters, see Section 5.1.3). Homogeneus halfspace with resistivity defined by average data resistivity was used as a starting model for all 3D inversions. The final 3D resistivity models were analyzed in

ParaView [35], where the computed volumes of the ramparts/ditch based on acquired resistivity boundaries were also extracted (function thresholds and integrated variables).

4. Results

4.1. Hillfort Hradišťany

All six 2D models (Figure 3A–F) show similar features; therefore, only profile P1 (Figure 3A) will be described in detail. At the center of the model, between 11 and 19 m, is an extremely high resistivity anomaly (>3000 Ωm, R1) with a thickness reaching down to 2 m. The near-surface parts of the model show high resistivities between 1000 and 3000 Ωm (R2) down to a depth of 2 m. Underneath is a layer with mid-resistivity around 100 Ωm (C1), from which two low-resistivity anomalies emerge (~40 Ωm, C2; ~20 Ωm, C3).

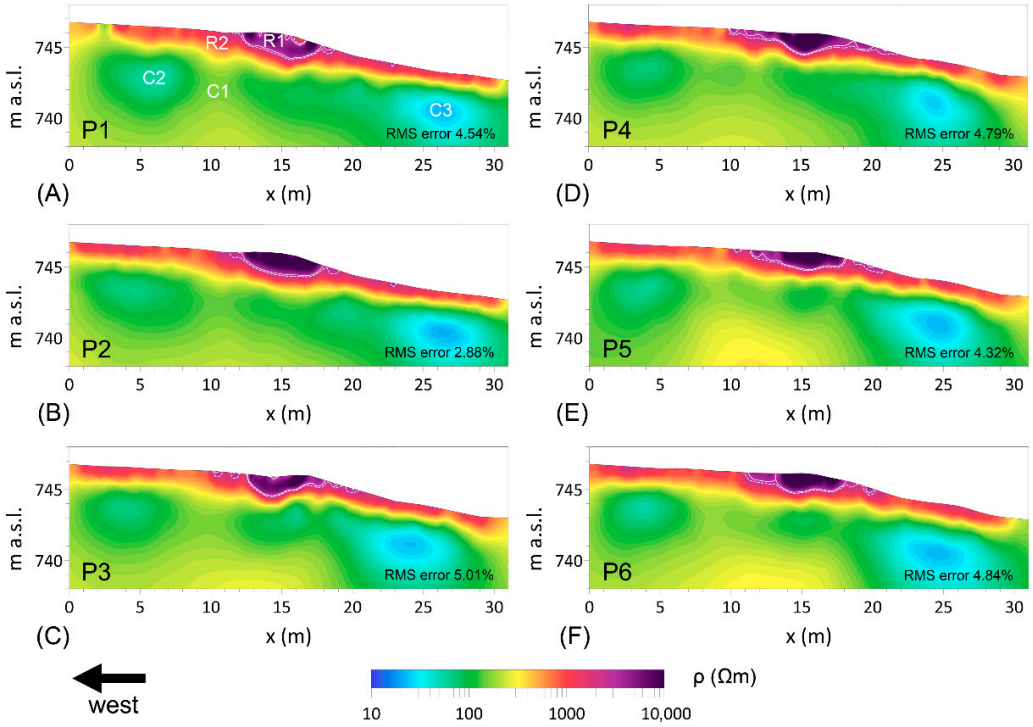

Figure 3. 2D inversion results for the ERT profiles from hillfort Hradišťany. (**A**–**F**) show profiles P1–P6 with a high-resistivity rampart (R1) delimited by a resistivity value of 2511 Ωm (white dashed line) and 3162 Ωm (white full line). The other marked anomalies are related to geology features: weathered volcanics (R2), sediments or weathered saturated volcanics (C1), unrecognized conductive anomalies (C2, C3) probably related to geology (for more details see Section 5.1.1).

4.2. Hillfort Královice

All five 2D models (Figure 4A–E) show similar results. In the middle of profiles P1–P4 and between 10 and 27 m is the elevated structure of the rampart with a layer of higher resistivity (>100 Ωm, R1) to a depth of around 1.5–2 m. To the east of the rampart is another high-resistivity anomaly (>200 Ωm, R2) down to a depth of 4 m. All profiles are from the surface to a depth of around 4 m, characterized by low resistivity layer (30–70 Ωm, C1), which is elevated under the rampart. Deeper parts of the profiles exhibit higher resistivities (100–200 Ωm, R3). The longer profile P5 shows the same anomalies and offers greater depth/horizontal range.

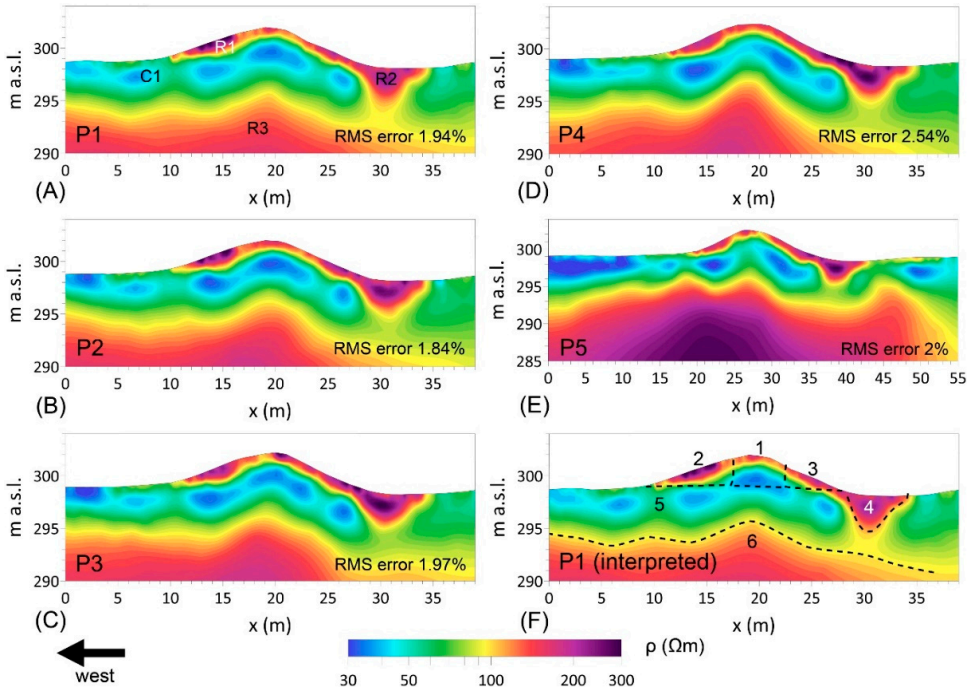

Figure 4. 2D inversion results for the ERT profiles from hillfort Královice. (**A**–**E**) show profiles P1–P5 with elevated rampart structure with mixed resistivities (R1), ditch (R2), quaternary loess (C1), and Proterozoic basement (R3). (**F**) shows interpreted profile P1 and displays individual parts of the rampart (1–3), ditch (4), quaternary loess (5), and Proterozoic basement (6; for more details see Section 5.2.1).

5. Discussion

5.1. Hillfort Hradišťany

5.1.1. Geophysical Interpretation

The resistivity model from the 3D inversion (Figure 5A) shows the resistivity structure of the defensive line in space—an extremely high-resistivity anomaly covering the middle of the profile with a mid-resistivity layer beneath, making it very similar to individual profiles. However, 2D models offer higher resistivity contrast; thus, we would rather interpret individual features using 2D results. All profiles from hillfort Hradišťany (Figure 3) clearly show ramparts built with dry-stacked stones (R1) emerging from the layer of weathered volcanics (R2). Underlying layer C1 could represent sediments of Most Fm., which were found on the acropolis [36]. However, layer C1 could also be related to weathered and saturated volcanics, which are expected on top of the former volcano. It is unclear what the lower-resistivity anomalies C2 and C3 represent; however, considering their depth, they could be linked to lower-resistivity intercalations within sediments/volcanics and have nothing to do with the former settlement.

5.1.2. Determination of Resistivity Boundary

Resistivity contrast between the dry-stacked stone building rampart and surrounding weathered volcanics is clearly visible on both 2D and 3D models. The surface manifestation of the rampart, which covered all six profiles between 11 and 19 m, was used to determine the resistivity boundary delineating the rampart. This part of the profile coincides well with a high-resistivity anomaly between 2511 Ωm (3.4 $\log_{10}$ Ωm) and 3162 Ωm (3.5 $\log_{10}$ Ωm).

We are aware that determining the strict resistivity value for defining rampart boundaries is not an easy task. The computed model is influenced by the nature of the geophysical method used and the processes that transformed the rampart into its current state. However, strong resistivity contrast defines the narrow range of resistivities representing the

searched boundary. Since both resistivities can identify the rampart structure, the volumetric information was retrieved for both values. Finally, the threshold of 3162 Ωm was used for interpretation due to above mentioned reasons.

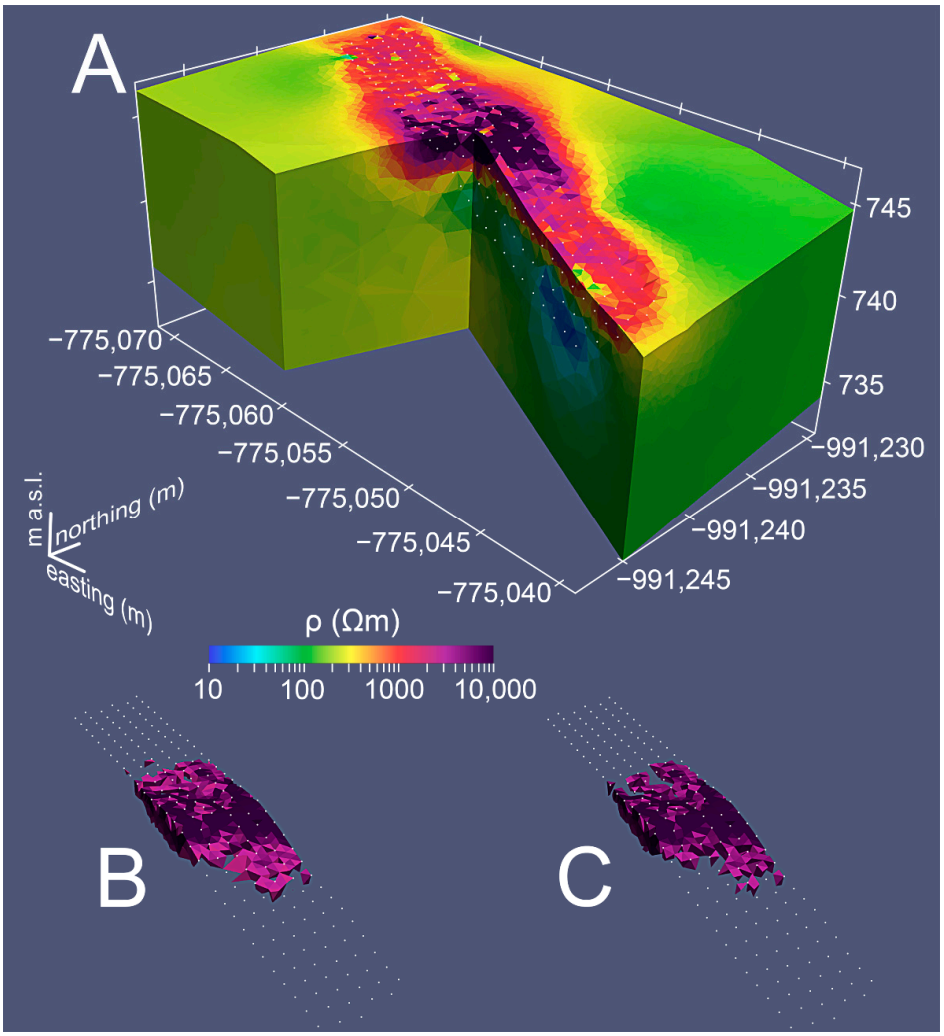

Figure 5. 3D inversion result for hillfort Hradištany (inversion run 3 with RMS error 4.46%): (**A**) Entire 3D model shows the resistivity distribution in decadic logarithms within S-JTSK/Krovak, Bpv coordinate frame. (**B**) Resistivity structure of the rampart when the threshold of 2511 Ωm (3.4 $\log_{10}$ Ωm) was applied. (**C**) Resistivity structure of the rampart when the threshold of 3162 Ωm (3.5 $\log_{10}$ Ωm) was applied. The white dots represent the individual positions of the electrodes. The zero position of each profile is located to the west.

5.1.3. Determination of Rampart Volume

When particular thresholds were applied to the 3D model, the lower resistivity of the 2511 Ωm elongated rampart structure exceeds the recorded surface manifestations (Figure 5B). The higher resistivity of the 3162 Ωm elongated rampart structure was significantly less (Figure 5C). This behavior is attributable to the destruction undergone by the rampart when its mass collapsed to the side over the years. Evidence of destruction is also seen in the resistivity anomaly positions related to rampart stones, mainly on the eastern side facing downhill. The idea that resistivities >2511 Ωm belong to rampart materials is supported because these resistivities are only found within surface manifestations of the rampart or on the eastern side of the rampart facing downhill. This finding implies that rampart stones are more likely delimited by a resistivity of 3162 than 2511 Ωm.

Once a threshold value for the rampart was chosen, a set of 3D inversions was calculated to explore how individual computational settings affect the resulting volume. We

conducted the entire analysis assuming that models with lower errors between the modeled and measured data are better and correspond well to the field situation. Afterward, we analyzed different inversion settings in detail: L1 vs. L2 norm, regularization strength, surface mesh quality, the cell size of the model, and smooth/robust constraints of the model (Table 1).

Table 1. Summary of 3D inversion runs performed for hillfort Hradišťany. The presented volumes are related to a 1-m-wide strip across the rampart and were computed as an average from the entire 5 m wide strip covered by 3D inversion.

Run	Inversion:	Max Surface Cell (m^2)	Max Cell Size (m^3)	Regularization Strength (Lambda)	Regularization Decrease (Each Iteration)	RMS Error (%)	Volume (m^3) 2511 Ωm	Volume (m^3) 3162 Ωm
1	L2	0.5	30	200	40%	5.12	9.504	9.046
2	L2	0.25	30	200	20%	5.24	8.126	7.092
3	L2	0.2	20	100	20%	4.46	8.102	6.76
4	L2	0.2	30	20	off	8.01	8.224	6.76
5	L1 + blocky	0.5	30	200	40%	15.08	6.844	5.006
6	L1 + blocky	0.2	30	20	off	19.08	7.932	6.4
7	L2 + blocky	0.2	30	20	off	6.09	7.98	6.91
8	L1	0.2	30	20	off	34.2	-	-

The inversion using the L2 norm favors smooth transitions and expects a Gaussian distribution of misfits; the L1 norm can be employed for significant outliers in the data. However, the L1 norm usually cause loose of resolution [31]. In addition, the blocky model can be used with both L1 and L2 norms to enhance resistivity contrasts within the model and overcome smooth transitions. Table 1 shows inversions using the L1 norm generally poorly fit data. Run 8 using the L1 norm with a disabled blocky model could not fit data and produced nonsense results. The standard L2 inversion produced results with an RMS error in the range 4.46–8.01%, even with the activated blocky model (run 7). Since L1 inversions exhibit larger misfits than the standard L2, the next paragraph in this article discusses setting changes only within smooth L2 inversions.

A significant factor that impacted the final volume was the size of the tetrahedrons comprising the 3D model, especially the maximum triangle-sized cells at the surface, i.e., the surface mesh quality. The larger cells render the model's surface coarser, and the data fit is usually worse. In addition, a coarse surface causes the total obtained volume to be larger due to an inability to construct the surface in the desired level of detail. The maximum cell size appears to have had only a minor influence on the volumetric information if set small enough, because it only affects cells at greater depths. Regularization controls the smoothness of the model (complexity) and directly affects model error—the smaller the regularization, the better the model represents the data. However, if the regularization is set too small, the model will likely cause overfitting, usually by the appearance of small-scale resistivity anomalies without any physical meaning. Furthermore, the regularization strength within the inversion process often decreases by approximately a certain percentage with every iteration. Runs 2–4 have similar settings, which suggest that regularization strength has only a minor effect on the total volume.

Considering only inversions using the L2 norm, the calculated volume of material in the 1-m-wide strip of rampart ranged roughly from 8 to 9.5 m^3 for a 2511 Ωm threshold and between 7 and 9 m^3 for a threshold of 3162 Ωm. If we accept that the value of 3162 Ωm is more accurate, Table 1 shows that runs 2, 3, 4, and 7 delivered similar volumes (7.092/6.76/6.76/6.91 m^3). Run 1 had the highest volume at 9.05 m^3, and run 5 had the

lowest volume at 5.01 m^3. Analyzing the RMS error, the best fit between the observed and modeled data was run 3, with a volume of 6.76 m^3.

5.2. Hillfort Královice

5.2.1. Geophysical Interpretation

The resistivity model from the 3D inversion (Figure 6A) shows the resistivity structure of defensive line in space, but as in the case of hillfort Hradišťany, the 2D profile will be interpreted. Only profile P1 from hillfort Královice in Figure 4F was interpreted due to the similarity between all measured profiles. The inverted cross-section showed the elevated rampart with mixed resistivities and the ditch on its eastern side. Due to previous archaeological excavations, individual building phases and the internal structure of the rampart could be inferred. The rampart's low-resistivity original core, built in phase one (1), is probably located between positions 16 and 21 m, where the resistivity confirms loess to be the main material of the rampart's core. Between positions 10 and 16 m, the rear earth ramp (2) is located, while in front of the rampart is the front earth ramp (3), both of which were accumulated during phase two. The higher resistivities correspond to an increased amount of rock found during the excavations. Furthermore, the front earth ramp may contain rock from a collapsed screen wall, which mainly fills the ditch (4). The low-resistivity layer from the surface to a depth of around 4 m may be related to the Quaternary loess (5), whereas the high-resistivity basement was built with Proterozoic sediments (6).

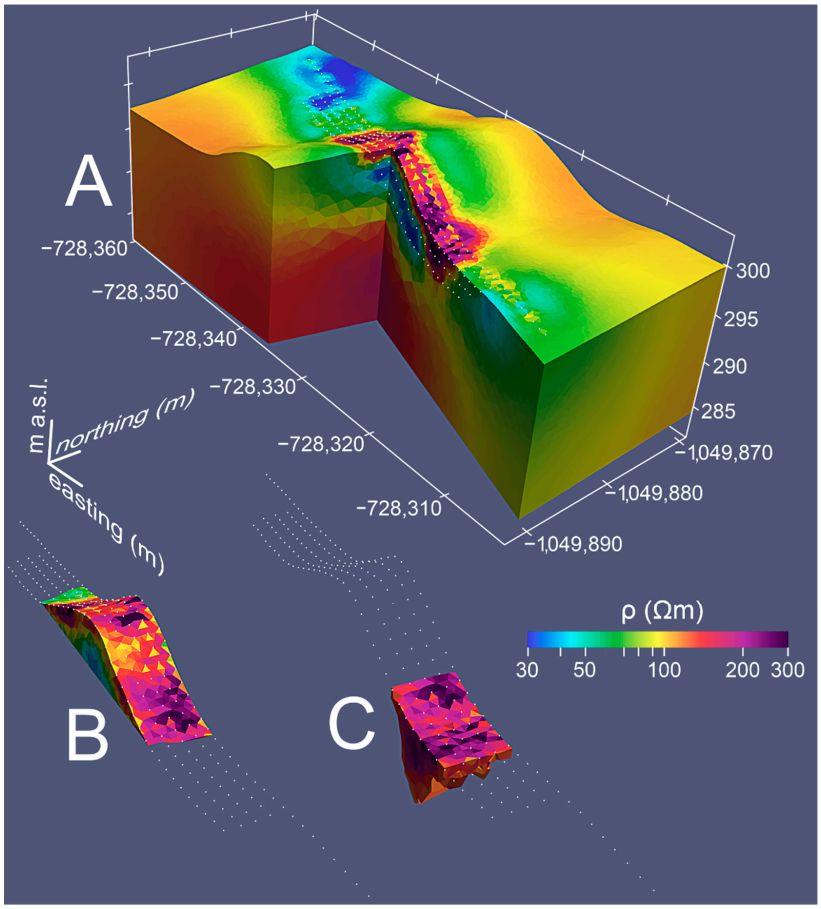

Figure 6. 3D inversion results from hillfort Královice (inversion run 3 with RMS error 2.82%). (**A**) Entire 3D model showing the distribution of resistivity in decadic logarithms within S-JTSK/Krovak, Bpv coordinate frame. (**B**) Isolated resistivity structure of rampart without any thresholds. (**C**) Resistivity structure of the ditch with a threshold of 126 Ωm (2.1 $\log_{10}$ Ωm) was applied. The white dots represent the individual positions of the electrodes. Zero position of the profiles is to the west.

5.2.2. Determination of Resistivity Boundary

The rampart showed mixed resistivities, and only its total volume could be estimated, because neither of the building phases could be exactly separated based on the resistivity image. According to excavations, the rampart was founded directly on the loess layer, which can be approximately identified from the 2D models. Consequently, the lower boundary of the rampart could be determined by the top of the loess layer and by the present continuing surface under the rampart's body. An inclined plane starting at an altitude of 288.8 m on profile P1 and ending at 299.1 m on profile P5 was used for the rampart's delimitation. The plane was also slightly inclined in the profile direction (Figure 6B).

The situation is different in the case of the ditch, which was dug into a low-resistivity loess layer and later filled by a high-resistivity material from the frontal screen wall together with material from the frontal earth ramp. The infill of the ditch's resistivity is in contrast with the surrounding loess, and its boundary can be assigned values from 104 Ωm (2.02 $\log_{10}$ Ωm) up to 126 Ωm (2.1 $\log_{10}$ Ωm) based on the 2D models. Due to the sharp contrast, these values are in agreement with the excavations, confirming that the ditch's base was ca. 4.2 m in depth.

5.2.3. Determination of Rampart/Ditch Volume

When estimated resistivity values were applied as a threshold to the 3D models, a value of 104 Ωm did not define the ditch itself; nonetheless, it still connects its anomaly to the high-resistivity basement. However, the value of 126 Ωm depicted only the high-resistivity structure of the ditch (Figure 6C), allowing us to compute ditch volume. Therefore, this value was considered a threshold for further evaluation.

The same methodology for volume determination used in the case of hillfort Hradišťany can be applied to hillfort Královice. Therefore, individual inversion parameters will not be discussed further. A set of 3D inversions (Table 2) delivered similar results for RMS error, the rampart's volume, and particularly for the ditch. Although the robust L1 inversion still performs worse than the standard L2 inversion, the distribution of the obtained volumes was quite uniform in the settings used. This finding was not surprising for the rampart, which was cut from the rest of the model by the same plane in every inversion run. The 1-m-wide strip of the rampart had a volume of ca. 38 m^3, whereas small volume variations were probably caused by a slightly different mesh generation or surface roughness. The volume of the ditch material ranged roughly between 12 and 16.3 m^3; if we exclude the L1 inversions, the volume range narrows to 14.7–16.3 m^3.

Table 2. Summary of 3D inversion runs within hillfort Královice. The presented volumes are related to a 1-m-wide strip across the rampart/ditch, and were computed as an average from the entire 4 m wide strip covered by 3D inversion.

Run	Inversion:	Max Surface Cell (m^2)	Max Cell Size (m^3)	Regularization Strength (Lambda)	Regularization Decrease (Each Iteration)	RMS Error (%)	Rampart Volume (m^3)	Ditch Volume (m^3)
1	L2	1	50	100	20%	2.83	38.015	14.74
2	L2	0.5	30	100	20%	2.97	37.63	15.43
3	L2	0.25	50	200	20%	2.82	37.73	16.3
4	L2 + blocky	0.5	50	200	20%	3.03	37.46	14.88
5	L1 + blocky	0.5	50	200	20%	5.97	37.84	14.68
6	L1	0.5	50	200	20%	3.03	37.61	12.2
7	L2	0.5	50	20	off	2.99	37.57	15.3

5.3. Applicability of the Presented Approach

The calculated volumes can be directly compared to archaeological information because excavations were performed on both sites. The rampart on hillfort Hradišťany was excavated in 1951, when the original width and height of the rampart were inferred at 3.3 m and more than 2 m, respectively [25,26]. These measurements imply that the 1-m-wide strip of rampart originally had a minimal volume of 6.6 m^3, which coincides well with the output of the 3D inversion run with the smallest RMS error delivering a volume of 6.76 m^3. Since the other four inversion runs provide similar values, we think these results may correspond to reality. We are aware that these numbers may be incorrect due to the selected resistivity threshold, different computational settings during ERT modeling or alternation of remains by erosional processes, etc., while the original amount of material was different from the preserved one. However, similar values obtained by the ERT modeling and archaeological study suggest that the 3D inversion can provide comparable results to direct excavations. The great advantage of ERT is its ability to image and model the buried part of the rampart, preventing the use of simple field measurement and mathematical formulae for the derivation of volumetric information.

In the case of the rampart within hillfort Královice, ERT provided the total volume of the rampart; however, due to mixed resistivities, it could not deliver the volume of individual building phases. It is possible, that better results could be achieved by smaller electrode spacing (e.g., 0.5 m) or by integrating other geophysical data (e.g., GPR). However, this has not been tested yet. Since the rampart was not buried and was found almost directly on the surface, the obtained volume of ca. 38 m^3 for the 1-m-wide strip is in agreement with simple field measurements and calculations using mathematical formulae, which provided a volume of 37.3 m^3. ERT does not offer any advantage in this case besides showing the internal structure of the rampart. In case of the ditch most of the inversion runs delivered a volume of 14.7–16.3 m^3 for the 1-m-wide strip. If we compare this value with the volume of the rampart's core, which was built in the first construction phase, the volume obtained by simple calculation is ca 14 m^3. Moreover, excavations suggest that the core of the rampart was built from a material dug from the ditch. This suggestion could mean that ERT proves that the amount of material used for building the rampart's core is roughly equal to the material dug from the ditch. Therefore, the ERT method can provide meaningful information even for ditches.

Examples from both sites show that through 3D ERT inversion, it is possible to obtain the volumetric information of defensive structures, which is truly beneficial for buried or semi-buried structures. Compared to excavations, ERT can estimate volume with more data. The wider the measured section of the rampart, the more accurate the averaged volume. In addition, ERT can be performed at a fraction of the cost and time. As a non-invasive tool, it also leaves the site intact compared with direct excavation.

5.4. Architectural Energetics Analysis

We estimated the labor cost based on the acquired structure volumes. The inner rampart of hillfort Hradišťany is 698 m long. If we consider the best inversion result, the volume of 1-m-wide strip would be 6.76 m^3, and the total volume of the entire rampart would be 4720 m^3. The rampart was built with local basalts based on petrographic analysis [37], forming the local rubble fields and suggesting that the builders did not have to transport material over longer distances. If we simplify the calculation and neglect the material transportation, we can determine the work rate for the stone quarrying of basaltic breccia by Murakami [38]. This study proposes a work rate of 0.66 m^3/p-d (person-day; see Section 1) for a 5 h working day, implying that gathering material for our rampart would take 7151 p-d. It is difficult to estimate the labor cost for building the dry-stacked stone wall, since all available estimates [38,39] discuss walls built with mortar/mud. If we assume the same work rate for gathering the materials (probably very conservative), the total labor cost of the rampart building is 14,302 p-d. With the involvement of 100 workers, the inner rampart could be constructed within approximately 144 days.

The situation at the hillfort Královice is more complex due to there being two building phases and the ramparts being structurally more complex. Therefore, we focused on the ditch from the first phase only, which was dug in loess. If we consider inversion run with the lowest RMS error, the 1 m part of ditch has a volume of 16.3 m^3, and the entire length of the ditch is 335 m, and the total volume of the ditch is 5460 m^3. According to grain classification diagrams [40], the loess is between the silt loam and clay/silty clay loam. We found a work rate for the silt and clay loam soil: 2.1 m^3/p-d (5 h working day; [41]). For more dense soils are working rates significantly lower [42]: 1.45 m^3/p-d (5 h working day); thus, a value above 2 m^3/p-d seems reasonable. If a 2.1 m^3/p-d rate was employed, digging the entire ditch would have been 2600 p-d. It would have taken approximately 26 days for 100 workers to dig the ditch. The same kind of analysis could have been performed for the rampart; however, this is a topic for a separate complex study due to its complicated structure.

6. Conclusions

ERT was used to estimate the volume of defensive structures, whereas inferred values were subsequently used for architectural energetics analysis. The results of our dense 3D survey processed through 3D inversion delivered meaningful volumes from two investigated hillforts of different ages, including ramparts from various materials and a ditch. ERT is beneficial for homogeneous buried or semi-buried structures such as deeply founded ramparts, since their actual volume can only be obtained by excavations. When compared to direct excavations, the 3D ERT models suggest that both methods lead to almost the same construction volumes. ERT is also applicable to ditches, which are usually filled with different materials from the surrounding on-site soil/sediments. The acquired volume of the ditch can be compared to the adjacent rampart's volume because materials from the ditch were used for emerging defensive ramparts in many cases. Our results showed that the ditch volume was almost exactly the same as the volume of the rampart. ERT can only deliver the total volume for heterogeneous ramparts built in multiple stages from different materials. However, even showing their internal structure can be valuable for archeologists. It is important to note that the ERT method leaves the site intact and provides volumetric information for a fraction of the cost and time compared with direct excavations. The presented approach should be easily adaptable for the volume estimation of other archaeological monuments, which are intended to be analyzed using architectural energetics.

Author Contributions: Conceptualization, R.K. and H.G.; methodology, R.K.; software, R.K.; validation, R.K. and J.Š.; formal analysis, R.K. and R.B.; investigation, R.K., R.B. and J.Š.; resources, R.K. and J.Š.; data curation, R.K. and R.B.; writing—original draft preparation, R.K.; writing—review and editing, R.K., H.G., J.Š. and R.B.; visualization, R.K.; supervision, R.K.; project administration, R.K. and H.G.; funding acquisition, H.G. All authors have read and agreed to the published version of the manuscript.

Funding: This work was supported by the INTER-EXCELLENCE program of the Ministry of Education, Youth and Sport of the Czech Republic (MEYS), grant no. LTC19029.

Data Availability Statement: All geophysical data presented here are available in standard industry formats from https://doi.org/10.17632/z7y4t6jmwb.1 (accessed on 6 April 2022).

Conflicts of Interest: The authors declare no conflict of interest.

References

1. Abrams, M.E.; McCurdy, L. Massive assumptions and Moundbuilders—The history, method, and relevance of architectural energetics. In *Architectural Energetics in Archaeology—Analytical Expansions and Global Explorations*; McCurdy, L., Abrams, E.M., Eds.; Routledge: London, UK, 2019.
2. Abrams, E.M. The Organization of Labor in Late Classic Copan, Honduras: The Energetics of Construction. Ph.D. Thesis, Pennsylvania State University, University Park, PA, USA, 1984.

3. Abrams, E.M. Economic specialization and construction personnel in Classic Period Copan, Honduras. *Am. Antiq.* **1987**, *52*, 485–499. [CrossRef]
4. Abrams, E.M. Architecture and energy: An evolutionary perspective. *Archaeol. Method Theory* **1989**, *1*, 47–88.
5. Adams, R.E.W.; Adams, J.J. Volumetric and stylistic reassessment of classic Maya sites in the Peten, Rio Bec, Chenes, and Puuc Hills. *Anc. Mesoam.* **2003**, *14*, 139–150. [CrossRef]
6. Davis, J.L.; Burks, J.; Abrams, E.M. Labor recruitment among tribal societies—An architectural energetic analysis of Serpent Mound, Ohio. In *Architectural Energetics in Archaeology—Analytical Expansions and Global Explorations*; McCurdy, L., Abrams, E.M., Eds.; Routledge: London, UK, 2019.
7. Akca, I.; Balkaya, C.; Pülz, A.; Alanyali, H.S.; Kaya, M.A. Integrated geophysical investigations to reconstruct the archaeological features in the episcopal district of Side (Antalya, Southern Turkey). *J. Appl. Geophys.* **2019**, *163*, 22–30. [CrossRef]
8. Hegyi, A.; Urdea, P.; Floca, C.; Ardelean, A.; Onaca, A. Mapping the subsurface structures of a lost medieval village in South-Western Romania by combining conventional geophysical methods. *Archaeol. Prospect.* **2018**, *26*, 21–32. [CrossRef]
9. Abedi, M.; Fournier, D.; Devriese, S.G.R.; Oldenburg, D.W. Integrated inversion of airborne geophysics over a structural geological unit: A case study for delineation of a porphyry copper zone in Iran. *J. Appl. Geophys.* **2018**, *152*, 188–202. [CrossRef]
10. Nowaczinski, E.; Schukraft, G.; Rassmann, K.; Hecht, S.; Texier, F.; Eitel, B.; Bubenzer, O. Geophysical–Geochemical Reconstruction of Ancient Population Size—The Early Bronze Age Settlement of Fidvár (Slovakia). *Archaeol. Prospect.* **2013**, *20*, 267–283. [CrossRef]
11. Tabbagh, A. Electrical Resistivity and Electromagnetism. In *Encyclopedia of Geoarchaeology*; Gilbert, A.S., Ed.; Springer Science & Business Media: Dordrecht, Germany, 2017.
12. Conyers, L.B. Ground Penetrating Radar. In *Encyclopedia of Geoarchaeology*; Gilbert, A.S., Ed.; Springer Science & Business Media: Dordrecht, Germany, 2017.
13. Leontarakis, K.; Apostolopoulos, G.V. Model Stacking (MOST) technique applied in cross-hole ERT field data for the detection of Thessaloniki ancient walls' depth. *J. Appl. Geophys.* **2013**, *93*, 101–113. [CrossRef]
14. Nowaczinski, E.; Schukraft, G.; Hecht, S.; Rassmann, K.; Bubenzer, O.; Eitel, B. A Multimethodological Approach for the Investigation of Archaeological Ditches—Exemplified by the Early Bronze Age Settlement of Fidvár Near Vráble (Slovakia). *Archaeol. Prospect.* **2012**, *19*, 281–295. [CrossRef]
15. Klanica, R.; Křivánek, R.; Grison, H.; Tábořík, P.; Šteffl, J. Capabilities and limitations of electrical resistivity tomography for mapping and surveying hillfort fortifications. *Archaeol. Prospect.* **2022**, 1–16. [CrossRef]
16. Hegyi, A.; Diaconescu, D.; Urdea, P.; Sarris, A.; Pisz, M.; Onaca, A. Using Geophysics to Characterize a Prehistoric Burial Mound in Romania. *Remote Sens.* **2021**, *13*, 842. [CrossRef]
17. Al-Saadi, O.S.; Schmidt, V.; Becken, M.; Fritsch, T. Very-high-resolution electrical resistivity imaging of buried foundations of a Roman villa near Nonnweiler, Germany. *Archaeol. Prospect.* **2017**, *25*, 1–10. [CrossRef]
18. Dahlin, T.; Zhou, B. A numerical comparison of 2D resistivity imaging with 10 electrode arrays. *Geophys. Prospect.* **2004**, *52*, 379–398. [CrossRef]
19. Loke, M.H.; Barker, R.D. Rapid least-squares inversion of apparent resistivity pseudosections using a quasi-Newton method. *Geophys. Prospect.* **1996**, *44*, 131–152. [CrossRef]
20. Loke, M.H.; Acworth, I.; Dahlin, T. A comparison of smooth and blocky inversion methods in 2-D electrical imaging surveys. *Explor. Geophys.* **2003**, *34*, 182–187. [CrossRef]
21. Cajz, V. Proposal of lithostratigraphy for the České středohoří Mts. Volcanics. *Věstník Českého Geol. Ust. Bull. Czech Geol. Surv.* **2000**, *75*, 7–16.
22. Cajz, V.; Rapprich, V.; Erban, V.; Pécskay, Z.; Radoň, M. Late Miocene volcanic activity in the České středohoří Mountains (Ohře/Eger Graben, northern Bohemia). *Geol. Carpathica* **2009**, *60*, 519–533. [CrossRef]
23. Čtverák, V.; Lutovský, M.; Slabina, M.; Smejtek, L. *Encyklopedie Hradišť v Čechách*; Libri: Praha, Czech Republic, 2003.
24. Smrž, Z. Knovízské hradiště Hradišťany (K.Ú. Mukov) v severozápadních Čechách. *Archeol. Ve Středních Cech.* **2011**, *15*, 267–277.
25. Šolle, M.; Váňa, Z. Nálezová Zpráva Uložená v Regionálním Muzeu v Teplicích, Fond Teplice, k. ú. Mukov—Hradišťany, Evid. pod č. 1951-0395. 1951.
26. Šolle, M. Knovízské hradiště Hradišťany u Bíliny. *Archeol. Rozhl.* **1952**, *4*, 483–485, 498–499.
27. Smrž, Z. Höhenlokalitäten der Knovízer Kultur in NW-Böhmen. *Památky Archeol.* **1995**, *86*, 38–80.
28. Štefan, I.; Hasil, J. The early medieval stronghold in Prague-Královice Results of the excavation of the outer fortification. *Archeol. Rozhl.* **2014**, *67*, 453–492.
29. Loke, M.H. Rapid 2-D Resistivity & IP Inversion Using the Least-Squares Method. RES2DINV User's Manual, Geotomo Software. 2020. Available online: www.geotomosoft.com (accessed on 2 September 2021).
30. CUZK (State Administration of Land Surveying and Cadastre). Digital Terrain Model of the Czech Republic of the 5th generation (DMR 5G). 2017. Available online: https://ags.cuzk.cz/av/ (accessed on 5 August 2021).
31. Günther, T.; Rücker, C. Boundless Electrical Resistivity Tomography BERT2—The User Tutorial. 2019. Available online: http://www.resistivity.net/download/bert-tutorial.pdf (accessed on 15 March 2022).
32. Günther, T.; Rücker, C.; Spitzer, K. Three-dimensional modelling and inversion of dc resistivity data incorporating topography—II. Inversion. *Geophys. J. Int.* **2006**, *166*, 506–517. [CrossRef]
33. Rücker, C.; Günther, T.; Spitzer, K. Three-dimensional modelling and inversion of dc resistivity data incorporating topography—I. Modelling. *Geophys. J. Int.* **2006**, *166*, 495–505. [CrossRef]

34. Lysdahl, A.K.; Bazin, S.; Christensen, C.; Ahrens, S.; Günther, T.; Pfaffhuber, A.A. Comparison between 2D and 3D ERT inversion for engineering site investigations—A case study from Oslo Harbour. *Near Surf. Geophys.* **2017**, *15*, 201–209. [CrossRef]
35. Ayachit, U. *The ParaView Guide: A Parallel Visualization Application*; Kitware: Chapel Hill, NC, USA, 2015; ISBN 978-1930934306.
36. Klanica, R.; Grison, H. Geofyzikální průzkum locality Hradišťany. In *Hradiště Hradišťany—Výsledky Archeologického Nedestruktivního Výzkumu (2017–2020)*; Šteffl, J., Hentschová, R., Eds.; Regionální Muzeum v Teplicích: Teplice, Czechia, 2021.
37. Šteffl, J. Výsledky nedestruktivního výzkumu. In *Hradiště Hradišťany—Výsledky Archeologického Nedestruktivního Výzkumu (2017–2020)*; Šteffl, J., Hentschová, R., Eds.; Regionální muzeum v Teplicích: Teplice, Czechia, 2021.
38. Murakami, T. Replicative construction experiments at Teotihuacan, Mexico: Assessing the duration and timing of monumental construction. *J. Field Archaeol.* **2015**, *40*, 263–282. [CrossRef]
39. Smailes, R. Building Chan Chan: A project management perspective. *Lat. Am. Antiq.* **2011**, *22*, 37–63. [CrossRef]
40. Lindner, H.; Lehmkuhl, F.; Zeeden, C. Spatial loess distribution in the eastern Carpathian Basin: A novel approach based on geoscientific maps and data. *J. Maps* **2017**, *13*, 173–181. [CrossRef]
41. Gillette, H. *Earthwork and Its Cost: A Handbook of Earth Excavation*; McGraw-Hill: New York, NY, USA, 1903.
42. Hammerstedt, S. Mississippian Construction, Labor, and Social Organization in Western Kentucky. Ph.D. Thesis, Pennsylvania State University, University Park, PA, USA, 2005.